Use of a metal 3D printed and instrumented dilatometer

Utilisation d'un dilatomètre en métal 3D imprimé et instrumenté

Hao Shen, Wim Haegeman, Herman Peiffer
Laboratory of Geotechnics, Department of Civil Engineering, Ghent University, Belgium, ShenHao.geo@Gmail.com

ABSTRACT: This paper describes the development of an instrumented dilatometer which is identical in dimensions and thus soil disturbance during penetration to the standard dilatometer introduced by Prof. Marchetti in 1980, except for the use of a rigid piston with a larger displacement up to 2.35 mm and instrumentation allowing measurements of full pressure-displacement curve and pore-water pressure at the piston center. The fabrication of this instrumented dilatometer was assisted by a novel metal 3D printing technique, which may provide further insight in improving other geotechnical testing apparatus. The new instrumented dilatometer was tested at a site of silty sand in Belgium, along with a DMT and a CPT located 1 m apart. Results show that the instrumented DMT can provide an opportunity to improve the estimation of lift-off pressure p_0, which is crucial to the DMT interpretation, ba sed on the judgement of the full expansion curve.

RÉSUMÉ : Cet article décrit le développement d'un dilatomètre instrumenté de dimensions identiques - et donc n'induisant pas de perturbations supplémentaires du sol pendant la pénétration - à celles du dilatomètre standard introduit par le Prof. Marchetti en 1980, à l'exception de l'utilisation d'un piston rigide avec un déplacement plus important jusqu'à 2,35 mm et de l'instrumentation permettant des mesures de la courbe pleine pression-déplacement et la pression de l'eau interstitielle au centre du piston. La fabrication de ce dilatomètre instrumenté a été assistée par une nouvelle technique d'impression 3D de métal, qui peut fournir des indications utiles pour améliorer d'autres appareils d'essai géotechnique. Le nouveau dilatomètre instrumenté a été testé sur un site de sable limoneux en Belgique, avec un DMT et un CPT distants de 1 m. Les résultats montrent que la courbe complète de dilatation obtenue avec le DMT instrumenté peut fournir une opportunité d'améliorer l'estimation de la pression de décollage p_0, qui est au centre de l'interprétation DMT.

KEYWORDS: DMT; instrumented DMT; metal 3D printing; lift-off pressure p_0; horizontal stress index K_D

1 INTRODUCTION

The flat dilatometer test (DMT) was developed and introduced by Professor Marchetti (Marchetti 1980) and has gained acceptance as a routine in-situ test in numerous parts of the world, due to its robustness, repeatability and simplicity. The dilatometer blade is 95 mm wide and 15 thick, with a 60 mm diameter flexible steel membrane located on one side of the blade. In principle, the dilatometer works as an electric switch (on/off) to signal the moments when the center of the membrane has moved 0.05 mm and 1.1 mm by means of inflation/deflation using nitrogen gas pressure. Two basic DMT parameters can be determined using the following formulae:

$$p_0 = 1.05(A - Z_m + \Delta A) - 0.05(B - Z_m - \Delta B) \quad (1)$$

$$p_1 = B - Z_m - \Delta B \quad (2)$$

where A is the pressure reading at 0.05 mm displacement, B is the pressure reading at 1.1 mm displacement, ΔA and ΔB are corrections determined by calibration, Z_m is gage zero offset.

Note that p_0 is conceptually the lift-off pressure and is calculated using a linear extrapolation from the B-pressure at 1.1 mm displacement through the A-pressure at 0.05 mm displacement to a zero displacement. Then p_0 can be normalized as the dimensionless horizontal stress index $K_D = (p_0 - u_0)/\sigma'_{vo}$, where u_0 is the hydrostatic pore pressure at the depth of testing and σ'_{vo} is the in-situ effective overburden stress at the depth of testing. Together with p_1, the material index $I_D = (p_1 - p_0)/(p_0 - u_0)$ and the dilatometer modulus $E_D = 34.7(p_1 - p_0)$ can be further derived (Marchetti et al. 2001). Therefore, it is seen that p_0 is crucial for identifying K_D, I_D, E_D and thus of paramount importance in the DMT interpretation based on these three DMT indices.

The definition of p_0 is established on assumption of the linear pressure-displacement relationship, which is not possible to check using the standard dilatometer. However, it is possible that the pressure-displacement curve is non-linear in some soils because of: 1) the increase in pressure reaches the strength of the soil, and the soil adjacent to the membrane yields with a plastic region spreading around the membrane cavity. So the soil response to the membrane expansion is elasto-plastic and non-linear, which has been usually observed from tests in soft cohesive soils (Benoit and Stetson 2003); 2) during the dilatometer blade penetration to a desired testing depth, the total horizontal stresses of the soil elements reaches maximum near the blade shoulder which is the geometrical transition point of the blade surface, and then decrease to around 0.6 times the maximum value at the membrane (Finno 1993). This unloading effect can be observed in 3D numerical modelling of the blade penetration process (Finno 1993; Kouretzis et al. 2015). Following this unloading phase, an initial elastic reloading phase during the membrane expansion is thus usually spotted in the DMT pressure-displacement curve (Akbar and Clarke 2001; Campanella and Robertson 1991; Stetson et al. 2003). In some cases, this reloading phase can go beyond 0.05 mm, then the pressure-displacement relationship is likely to be non-linear between the A-pressure and the B-pressure since the initial elastic reloading is normally stiffer than the ensuing phase. Both issues can lead to noticeable errors using Eq. (1) to obtain p_0, however, it is technically infeasible to reduce these potential errors without modifying the standard dilatometer blade.

A number of modified dilatometers have been prototyped for different purposes, these modifications have been reviewed (Shen et al. 2015). Based on the experience gained in these prior apparatuses, an instrumented dilatometer prototype is developed to capture non-linear soil behavior during tests in a calibration chamber (Shen et al. 2016a). This paper describes further development of a more robust (metal 3D printed) dilatometer blade with instrumentation to allow not only the full DMT pressure-displacement curve but also the pore-water pressure and the thrust during penetration to be measured during field testing. These measurements are supposed to allow

an improvement of interpretation such as the determination of p_0 by reducing the aforementioned potential errors. Typical data in a silty sand site are presented and compared with standard DMT data and CPT data.

2 DESIGN OF AN INSTRUMENTED DILATOMETER

2 .1 *Metal 3D printing an instrumented dilatometer for in-situ testing*

To keep the same level of soil disturbance during the penetration stage, the new instrumented dilatometer blade complies with the nominal dimensions of the standard dilatometer blade which are 95 mm wide, 15 mm thick and 50 mm long in tapered section. However, in the following expansion stage, a 40 mm diameter rigid piston is used as the loading element instead of the flexible membrane, since the rigid piston can allow a larger displacement and easier integration of the pore-water intake filter at its center.

In Figure 1, the instrumented dilatometer is presented in an exploded view. Generally, the dilatometer comprises three chambers for different purposes: the one close to the blade tip is configured to house a displaceable rigid piston and an inductive distance sensor to measure the piston displacement; the middle chamber is a pore-water pressure cell comprising a pressure sensor and a tunnel connecting to the piston chamber; the third one is used to provide space during assembly and maintenance. Given the complexity of this instrumented dilatometer design, fabrication is challenging and even impossible in details like hidden grooves and irregular tunnels inside the blade using any standard machining tool. In a comparison, metal 3D printing technique does not suffer geometrical complexity and can significantly reduce the fabrication to a couple of days. But 3D printing technologies generally require a minimal thickness of printed objects to achieve its normal mechanical performance due to its layer-upon-layer printing process. Taking this into account, the printed dilatometer tip and the printed threads on the rod-blade connector cannot withstand the downward thrust during the penetration. Therefore, a hybrid fabrication strategy was used: the main blade body and the piston were metal 3D printed; the blade tip, the rod-blade connector and the covers were machined; then the parts were welded together using electrode CuSi3 as filler. Specifically, the used metal 3D printing technique is Binder Jetting (BJ) in 420 stainless steel infiltrated with bronze, which costs approximately € 300, and the finished parts compose of 60% stainless steel and 40% bronze infiltrant.

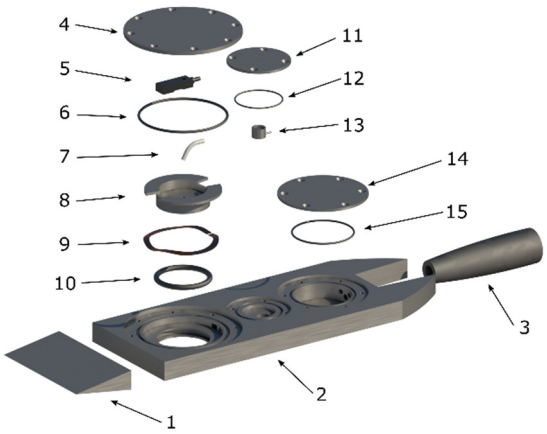

1	Blade tip	**9**	Wave spring
2	Main blade body	**10**	O-ring
3	Rod-blade connector	**11**	Cover
4	Cover	**12**	O-ring
5	Displacement sensor	**13**	Pore-water pressure sensor
6	O-ring	**14**	Cover
7	Drainage lead	**15**	O-ring
8	Rigid piston		

Figure 1. CAD-generated exploded view of the instrumented dilatometer

Figure 2(a) shows the fabricated instrumented dilatometer performing a calibration in air with the piston displacement up to 2.35 mm. Figure 2(c) illustrates the moment prior to the penetration stage in field testing, with the instrumented dilatometer blade mounted on push rods.

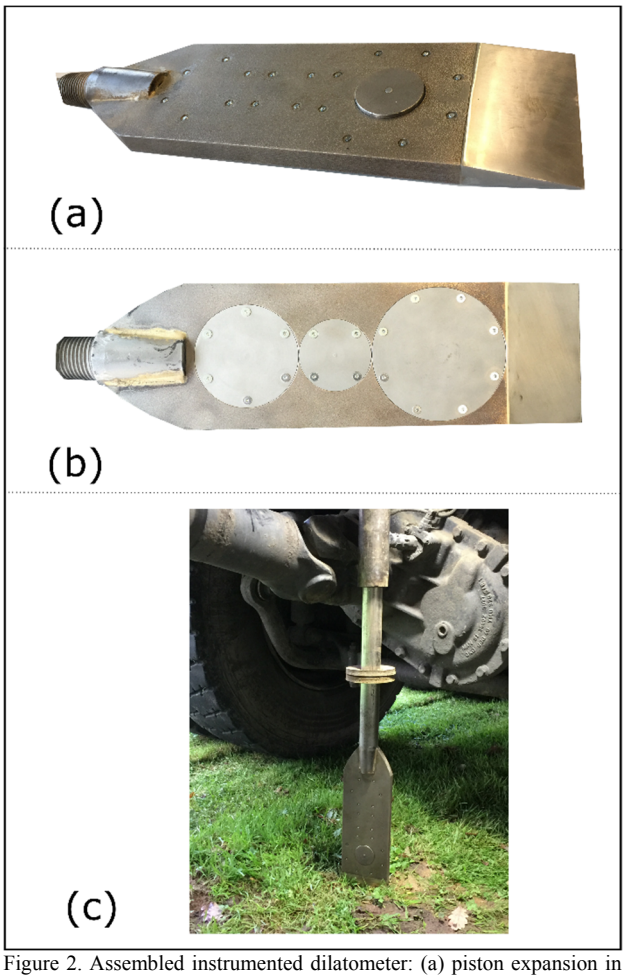

Figure 2. Assembled instrumented dilatometer: (a) piston expansion in an angled view; (b) bottom view; (c) assembled with a truck-based penetrometer.

2 .2 *Calibration*

Note that raw data from the instrumented dilatometer tests consists of not only soil response but also force exerted by the wave spring and friction of the O-ring. To determine the amount of these factors, it was decided to perform calibrations in air and adopt the same pressurization/depressurization rate as the field tests. Figure 3 shows a calibration carried out with monotonic loading and unloading rate. Two 4-order polynomial functions are fitted to loading and unloading curves, respectively. Then during correction of the raw data, a subtraction can be readily made using the fitted polynomial functions. Note that this calibration is carried out before and after a sounding to check consistence of the results.

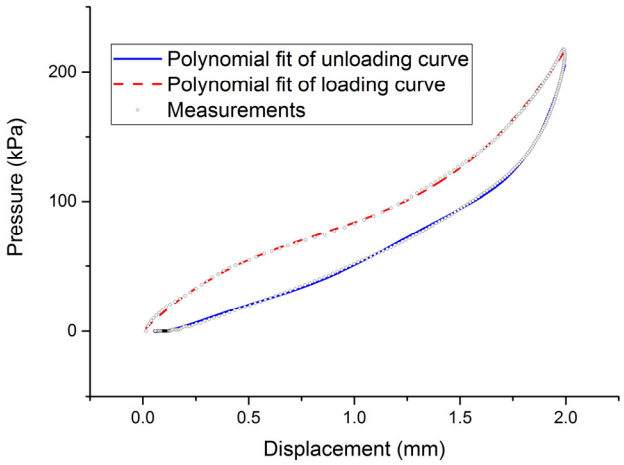

Figure 3. Calibration performed in air and polynomial curve fitting

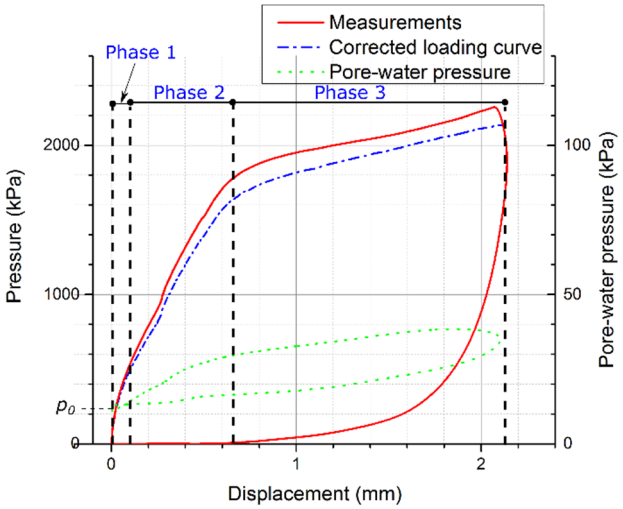

Figure 4. Typical testing curve at a depth of 4.0 m

3 FIELD TESTING

A field-testing program using the new instrumented dilatometer, a standard dilatometer and a 15 cm^2 piezocone is conducted at Ghent University located at Technologiepark, Zwijnaarde in Belgium, during October 2016 to November 2016. These three tests of different types are located 1 m apart from each other in an equilateral triangular pattern. This site is composed of about 2.5 m of sand over about 7.5 m of silty sand. During this testing program the groundwater table is about 2.8 m below ground surface.

A testing procedure is devised to minimize difference from the standard dilatometer testing procedure to allow a comparison between testing results. The instrumented dilatometer is installed using the same cone truck for the CPT and the DMT, with identical penetration rate of 2 cm/s. Once the piston reaches the desired testing depth, pressurization starts immediately. The loading rate is within the same range as that of the standard DMT, in terms of cavity volume per time. The cavity volume of the piston and the membrane is calculated as an expanding cylindrical element and an expanding spherical cap, respectively. The pressurization continues until at least a piston displacement of 2.0 mm or a pressure of 3.4 MPa (the maximum capacity of system) before an immediate depressurization. Though the instrumented dilatometer is capable of carrying out additional unload-reload (or reload-unload) loops to enhance estimation of soil stiffness, this is not adopted in this test to prevent influence on the comparison with the standard dilatometer. Before the penetration, the pore-water pressure cell and the pore-water intake filter at the piston center are fully saturated using viscous silicone oil. During the penetration stage, the thrust on top of the rods is measured by a load cell and a friction reducer is installed just above the blade, which allows an estimation of penetration resistance considering negligible friction on the rods.

3 .1 *Typical testing curve*

Figure 4 demonstrates typical good quality instrumented dilatometer data at a depth of 4.0 m. Raw data is firstly corrected using the polynomial fits from the calibration data, a corrected loading curve is thus produced to represent soil response for interpretation.

The piston begins to move outward when the pressure reaches around 100 kPa. The initial expansion curve is expected as a reloading soil response due to the unloading effects during the penetration stage. However, it is by no means possible to quantify the magnitude of this reloading stage (hereinafter phase 1) prior to testing. In the standard DMT, a prefixed displacement of 0.05 mm is used in the linear back extrapolation of p_0, which in fact neglects phase 1 occurring under 0.05 mm. It is therefore interesting to note that the conceptual lift-off pressure p_0 may not correspond to the de facto piston/membrane lift-off.

In the following phase, the piston is further pressurized and the soils respond linear but not as stiff as the preceding phase. This stage may be regarded as a pseudo-elastic phase (hereinafter phase 2) prior to the onset of plastic behavior. In this curve for a silty sand, phase 2 starts at around 0.08 mm until the initiation of yielding at about 0.65 mm.

As soon as the increase in pressure reaches the strength of the soils adjacent to the piston, phase 3 starts with non-linear and plastic soil response. It also appears that a limiting pressure is approached. Followed by a depressurization stage, phase 3 ends at 2.08 mm displacement, however, the maximum displacement of 2.13 mm is reached during the depressurization. This implies time-dependent deformations such as soil creep. Furthermore, pore-water pressure is measured through the test at the piston center and shows a slight increase above the equilibrium water pressure during the expansion and a gentle decline before reaching the max. displacement. This is possibly due to the generation of excess pore-water pressure to some extent while the dissipation in the same order of magnitude at the meantime is expected as well.

3 .2 *Estimation of the horizontal stress index* K_D

A deformation model for the piston cavity expansion and for the membrane cavity expansion is apparently different, which resembles a rigid/flexible footing sitting on an elastic half-space, subject to the condition of zero settlement external to the footing. However, in principle, the conceptual lift-off pressure p_0 at zero displacement is not influenced by this difference between the piston and the membrane expansion.

In the standard dilatometer, p_0 is estimated by a linear extrapolation through pressure readings at prefixed displacement levels of 0.05 mm and 1.1 mm. In the instrumented dilatometer, the determination of p_0 can be assisted by checking the different pressure-displacement curves in each test.

This involves firstly identifying the proposed three phases of the expansion curve. Then only the phase 2 of the loading curve is adopted to back-extrapolate p_0 at zero displacement, using a linear regression. This method can prevent potential errors including parts of phase 1 or 3 in the prefixed displacement range such as that of the standard dilatometer. Note that in this test, phase 2 covers an approximate range of 0.55 mm displacement.

To allow a comparison between different testing results, the normalized form of p_0 (K_D) is thus used. Figure 5 presents a

comparison of K_D estimated by the instrumented DMT and the standard DMT. In addition, K_D is predicted out of CPT data using the following correlation for sand-like soils (Robertson 2009):

$$K_D = (\alpha/34.7) \cdot Q_{t1} / \left[10^{(1.67-0.67I_C)}\right] \quad (3)$$

where $2 < \alpha < 10$ depends on soil type, relative density, age and stress history; Q_{t1}= the normalized cone resistance; I_C= the soil behavior type index.

In general, the comparison between K_D estimated by the instrumented DMT and the standard DMT shows reasonable trends. The large variation in K_D between 1 and 2.5 m, from crust to subsoils, is fairly captured by the instrumented DMT. The instrumented DMT estimates smaller variation between 4.5 to 6.2 m than that of the standard DMT. As an adjacent CPT result is available, the CPT predicted K_D values are presented in a band bounded by two curves, since the correlation for sand-like soils is only approximate and depends on α which is 2.1 and 5.6 for the two boundaries in this diagram. It is interesting to note that those measured K_D values tend to get close to the lower bound between 2 and 4.5 m while to approach the upper band between 4.5 and 7m.

It is important to note that the method of linear extrapolation of phase 2 for p_0 interpretation is proposed only based on the data in silty sand. The effective stress is dominant in the soil response during the penetration as well as the piston expansion. However, p_0 can be dominated by the excess pore-water pressure adjacent to the membrane in soft clays (Campanella and Robertson 1991; Mayne 2006). This can present difficulties to use this method as phase 2 is usually non-linear and transitional in curves under this condition. An alternative method is suggested to address this type of smooth curves (Shen et al. 2016b). Hence, it appears that p_0 determination based on the full pressure-displacement curve will not be unique for all soils because of various types of curves. However, the identification of three phases in the expansion curve may form a framework for future refinements and help estimation of soil parameters.

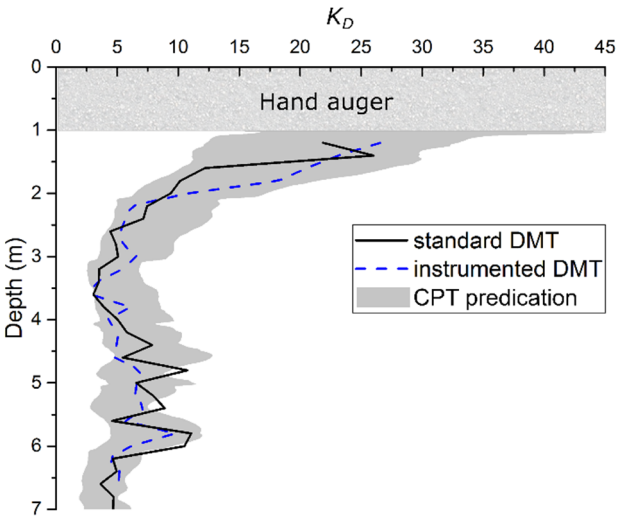

Figure 5. Comparison of horizontal stress index K_D: estimated by DMT and iDMT results, predicted out of CPT results.

4 CONCLUSION

The standard DMT has been used in many parts of the world over 30 years. The lift-off pressure p_0 is fundamental in the interpretation of soil parameters. Although the p_0 interpreted using the standard DMT is simple and repeatable, the estimation of p_0 can still be improved with the full expansion curve and the pore-water pressure measurements. Thus a new instrumented DMT is developed to achieve this objective. The fabrication of the instrumented dilatometer is assisted by the metal 3D printing technique to allow a piston displacement up to 2.35 mm and pore-water pressure measurements at the piston center.

Recently, one CPT, one DMT and one new instrumented DMT are carried out at adjacent locations only 1m apart each other at a silty sand site in Belgium. From the expansion curve of the instrumented DMT, it is possible to generally identify three loading phases, which starts with an initial reloading phase 1, then a pseudo-elastic phase 2 and finally a plastic phase 3. The p_0 interpretation is based on a linear back-extrapolation of phase 2 for this test. Comparison of the normalized form of p_0 (K_D) between the instrumented DMT, the DMT and the CPT predications shows reasonable trends, considering the variations in soil stratigraphy and consistency in such a silty sand deposit. However, it is necessary to note that the data discussed in this paper is based on a site of silty sand. Further research and tests in various soil conditions are required to develop a unified p_0 interpretation technique based on the full expansion curve.

5 ACKNOWLEDGEMENTS

The first author acknowledges the financial support from the program of China Scholarships Council (No. 201306320157). Without the valuable support from Geosonda, especially Jeroen Jacobs who operated the field equipment, the in-situ tests cannot be accomplished.

6 REFERENCES

Akbar, A., and Clarke, B. G. 2001. A flat dilatometer to operate in glacial tills. *Geotechnical Testing Journal* 24(1), 51–60.

Benoit, J., and Stetson, K. P. 2003. Use of an instrumented flat dilatometer in soft varved clay. *Journal of geotechnical and geoenvironmental engineering* 129(12), 1159–1167.

Campanella, R. G., and Robertson, P. K. 1991. Use and interpretation of a research dilatometer. *Canadian Geotechnical Journal* 28(1), 113–126.

Finno, R. J. 1993. Analytical interpretation of dilatometer penetration through saturated cohesive soils. *Geotechnique* 43(2), 241–254.

Kouretzis, G. P., Ansari, Y., Pineda, J., Kelly, R., and Sheng, D. 2015. Numerical evaluation of clay disturbance during blade penetration in the flat dilatometer test. *Géotechnique Letters* 5, 91–95.

Marchetti, S. 1980. *In-situ tests by flat dilatometer. Journal of the Geotechnical Engineering Division* 106(3), 299–321.

Marchetti, S., Monaco, P., Totani, G., and Calabrese, M. 2001. The flat dilatometer test (DMT) in soil investigations. *International Conference on In-situ Measurement of Soil Properties*, Bali, 95–131.

Mayne, P. W. 2006. Interrelationships of DMT and CPT readings in soft clays. *Proceedings from the Second International Flat Dilatometer Conference*, Atlanta, 220–225.

Robertson, P. K. 2009. CPT-DMT Correlations. *Journal of Geotechnical and Geoenvironmental Engineering* 135(11), 1762–1771.

Shen, H., Haegeman, W., and Peiffer, H. 2015. Instrumented DMT: Review and Analysis. *The 3rd International Conference on the Flat Dilatometer*, Rome, 377–384.

Shen, H., Haegeman, W., and Peiffer, H. 2016a. 3D Printing of an Instrumented DMT: Design, Development, and Initial Testing. *Geotechnical Testing Journal* 39(3), 492–499.

Shen, H., Haegeman, W., and Peiffer, H. 2016b. Interpretation of the instrumented DMT (iDMT): a more accurate estimation of p_0. *5th International Conference on Geotechnical and Geophysical Site Characterisation,* Gold Coast (in print).

Stetson, K. P., Benoit, J., and Carter, M. J. 2003. Design of an instrumented flat dilatometer. *Geotechnical Testing Journal* 26(3), 302–309